Photoluminescence properties of multilayer oxide films intercalated with rare earth ions by the layer-by-layer technique†

Shintaro Ida,* Kazuhiko Araki, Ugur Unal, Kazuyoshi Izawa, Ozge Altuntasoglu, Chikako Ogata and Yasumichi Matsumoto

Received (in Cambridge, UK) 28th March 2006, Accepted 22nd June 2006
First published as an Advance Article on the web 24th July 2006
DOI: 10.1039/b604451d

Multilayer oxide films consisting of a TiO–Eu^{3+}–TiO–Tb^{3+}–NbO–Tb^{3+}–NbO–Eu^{3+} unit which was prepared by the layer-by-layer technique, showed photoluminescence with a high intensity containing both red and green lights.

Layered oxides such as $Cs_{0.76}Ti_{1.81}O_4$, $K_2Ti_4O_9$ and $K_4Nb_6O_{17}$ are able to be exfoliated by an intercalation reaction.[1–3] Exfoliated layered oxides are called nanosheets, which have a thickness in the order of nanometres with a length and width in the order of micrometres. The exfoliated layered oxides have attracted much attention as a building block to assemble nanostructured films. Nanosheets with negative charges are dispersed in an aqueous solution. Mixing the nanosheets and cationic species results in reassembly according to the electrostatic aggregation, which is called the electrostatic self-assembly deposition (ESD) technique.[4] As another reassembly method, the layer-by-layer (LBL) assembly technique is reported.[5–7] By building up the nanosheets and ionic species with the LBL technique, new layered oxides that cannot be prepared with conventional solid-state methods can be created at room temperature. Many groups have reported layered films reassembled from nanosheets because of the expectation for various applications such as photocatalysts, batteries, semiconductor devices and optical devices.

Our interest is directed towards developing optical devices made of nanosheets. So far, the titanate layered oxides intercalated with Eu^{3+} ions prepared by electrostatic self-assembly deposition exhibit red luminescence at room temperature by energy transfer from the nanosheets to Eu^{3+} ions, which is based on the nanosheet band gap excitation.[8,9] If layered oxides intercalated with various photoluminescent species exhibiting red, green and blue emissions are created by the LBL technique using nanosheets, white luminescence will be obtained from an ultra thin film. Thus, the layered oxides assembled from nanosheets have a tremendous amount of potential as luminescent materials. However, there are only a few studies on the photoluminescence of layered oxide films of nanosheets intercalated with luminescent species. In this paper, we report the photoluminescence properties of the layered oxide films of heterogeneous nanosheets intercalated with rare earth ions prepared by the LBL technique. The emission properties of the layered oxide films are strongly dependent on the combination of nanosheets and rare earth ions. The emission of Eu^{3+} in the interlayer region of the $Ti_{1.81}O_4$-sheets was stronger than that from the interlayer regions of Ti_4O_9-sheets and Nb_6O_{17}-sheets, while the emission of Tb^{3+} in the interlayer region of Nb_6O_{17}-sheets was stronger than that from the interlayer region of $Ti_{1.81}O_4$-sheets and Ti_4O_9-sheets. The red and green luminescence was obtained from the layered film of alternating titanate and niobate nanosheets intercalated with Eu^{3+} and Tb^{3+} ions as shown in Fig. 1.

$Cs_{0.76}Ti_{1.81}O_4$ (CTO), $K_2Ti_4O_9$ (KTO) and $K_4Nb_6O_{17}$ (KNO) were used as starting materials for the preparation of titanate or niobate nanosheets. CTO, which has some vacancies in the matrix,[1] was prepared by a complex polymerization method.[9] KTO and KNO were prepared by conventional solid-state reactions. Acetate salts of europium and terbium cations were used without any further treatment. Nanosheets were prepared by the protonation and exfoliation of the CTO, KTO and KNO. Nanosheets derived from CTO, KTO and KNO are abbreviated as $Ti_{1.81}O_4$-sheets, Ti_4O_9-sheets and Nb_6O_{17}-sheets. Preparation of the layered films by the LBL technique was carried out as follows. Platinum was used as a substrate in this study. Substrates were primed in an aqueous polyethyleneimine (PEI) 2.5 g L^{-1} solution for 20 min to charge the surface of the substrate positively. Primed substrates were dipped into the colloidal solution of negatively charged nanosheets and then 0.01 M aqueous $RE(CH_3COO)_3$ (RE = Eu, Tb) solution for 10 min repeatedly with rinsing and drying under a N_2 stream. The sequence was repeated *n* times. The layered oxides of nanosheets intercalated with rare earth ions (RE^{3+}) are described as $[RE\text{–nanosheet}]_n$. Excitation and emission spectra were analyzed by Jasco FP-6500 spectrofluorometer with a 150 W Xe lamp source. UV-vis absorption spectra of the deposited oxides were measured by an UV-vis spectrometer (Jasco V-550).

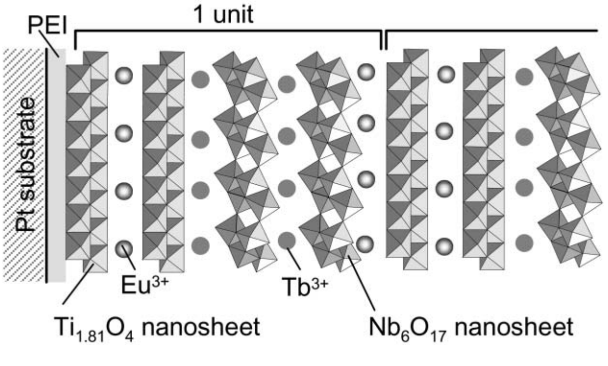

Fig. 1 Structure of the multilayer film intercalated with Eu^{3+} and Tb^{3+} ions.

Department of Applied Chemistry and Biochemistry, Faculty of Engineering, Kumamoto University, Kurokami 2-39-1, Kumamoto 860-8555, Japan. E-mail: s_ida@chem.chem.kumamoto-u.ac.jp; Fax: +81-96-342-3679; Tel: +81-342-3659

† Electronic supplementary information (ESI) available: AFM images. See DOI: 10.1039/b604451d

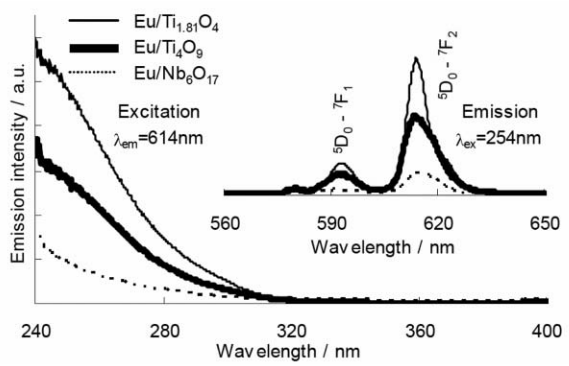

Fig. 2 Excitation and emission spectra of the [Eu–nanosheets]$_6$.

The thicknesses of the $Ti_{1.81}O_4$-sheets, Ti_4O_9-sheets and Nb_6O_{17}-sheets obtained by AFM observation were 0.87, 1.18 and 1.03 nm, respectively, indicating that monolayer nanosheets were successfully prepared. The theoretical thickness was smaller than the observed thickness of nanosheets because H_2O was adsorbed on the nanosheets under the AFM measurement environment.

The room temperature excitation and emission spectra of [Eu–nanosheets]$_n$ (n = 6) are shown in Fig. 2, where the excitation spectra were obtained by monitoring at 614 nm and the emission spectra were measured with an excitation wavelength of 254 nm. It was found that the emission of Eu–$Ti_{1.81}O_4$ was the strongest of the samples. The most intense emission peaks were observed at around 614 nm, which were assigned to the $^5D_0$–$^7F_2$ electric dipole transition. The second most intense peaks were observed at around 592 nm, which were assigned to the $^5D_0$–$^7F_1$ magnetic dipole transition. The excitation peaks were observed in the region below 320 nm. The peak at around 395 nm assigned to the intra-4f transition of the Eu^{3+} ion was not observed. It was indicated that the most intense emission of Eu^{3+} was attributable to the energy transfer from the nanosheets to Eu^{3+}.

Fig. 3 shows the room temperature emission and excitation spectra of [Tb–nanosheet]$_n$ (n = 6). The excitation wavelengths were 254 nm. In the case of the Tb–nanosheet, the green emission intensity of Tb–Nb_6O_{17} (dotted line) was the strongest of the three samples and that of Tb–$Ti_{1.81}O_4$ was much lower. The emission peaks from 480 to 650 nm were associated with the $^5D_4$–^7F_J (J = 3–6) transition. In the emission peaks, the green $^5D_4$–$^7F_5$ emission at around 545 nm was the strongest. The excitation spectrum of Tb–Nb_6O_{17} was the same as the UV-vis absorption spectra, indicating that the observed emission is mainly contributed to by the band gap excitation in the host nanosheet layer. Thus, in Tb–Nb_6O_{17} as well as Eu–$Ti_{1.81}O_4$, the energy produced by the band gap excitation migrates in the host layer and easily moves into the interlayer region, to be trapped by the Tb^{3+} cations.

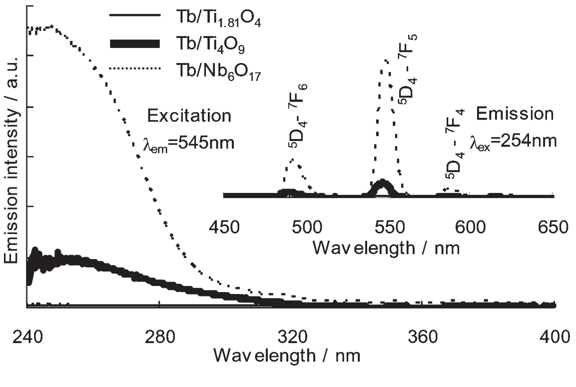

Fig. 3 Excitation and emission spectra of the [Tb–nanosheets]$_6$.

With regards to the emission mechanism of Eu^{3+} and Tb^{3+} between the nanosheets, it is reported that the energy transfer takes place when the defect state levels of the nanosheet are equal to or higher in energy than the excitation levels of rare earth ions, while no energy transfer takes place when the defect state levels of the nanosheet are lower than the excitation levels of the rare earth ions.[8–10] The reason why emissions of Eu^{3+} were observed from all samples is because the defect state levels of the $Ti_{1.81}O_4$-sheet, Ti_4O_9-sheet and Nb_6O_{17}-sheet were greater than the excitation levels of the Eu^{3+} ions. In comparison, the reason why much lower emissions of Tb^{3+} were observed from Tb–$Ti_{1.81}O_4$ might be because the defect state level of the $Ti_{1.81}O_4$-sheet is lower than the excitation levels of the Tb^{3+} ions. In addition, the defect state level of the Ti_4O_9-sheet might be higher than that of the $Ti_{1.81}O_4$-sheet.

From these results, it was found that emissions of Eu^{3+} and Tb^{3+} were stronger in the $Ti_{1.81}O_4$-sheet and Nb_6O_{17}-sheet interlayer region, respectively. Therefore, we tried to prepare the heterogeneous layered film, [$Ti_{1.81}O_4$–Eu–$Ti_{1.81}O_4$–Tb–Nb_6O_{17}–Tb–Nb_6O_{17}–Eu]$_n$, as shown in Fig. 1, to obtain the red and green emissions from an ultrathin film at once. The [$Ti_{1.81}O_4$–Eu–$Ti_{1.81}O_4$–Tb–Nb_6O_{17}–Tb–Nb_6O_{17}–Eu]$_n$ film is described as [Tb–Eu–multi-sheet]$_n$.

Fig. 4 shows the UV-vis absorption spectra of [Eu–$Ti_{1.81}O_4$]$_n$, [Tb–Nb_6O_{17}]$_n$ and [Tb–Eu–multi-sheet]$_n$. The sequence was repeated 1–6 times. As shown in Fig. 4, the absorption intensities were increased with increasing sequence number. This result indicates that the nanosheets were able to be deposited on the substrates. The peaks in the region of 200–400 nm were assigned to the absorbance by nanosheets. In the spectra of [Tb–Eu–multi-sheet]$_n$ (n = 1–3), two peaks, 231 and 294 nm in the region of 200–320 nm were assigned to the $Ti_{1.81}O_4$-sheet and Nb_6O_{17}-sheet, respectively. The chemical composition of the [Eu–Tb–multi-sheet]$_3$ film obtained by ICP measurement was Eu : Tb : Ti : Nb = 0.55 : 0.47 : 3.05 : 1.70. This chemical composition shows about a 25% excess amount of cation species, Eu^{3+} and Tb^{3+}, compared to the amount of cation species neutralizing the negative charge of [$Ti_{1.81}O_4$-sheet]$^{0.76-}$ and [Nb_6O_{17}-sheet]$^{4-}$. The excess amount of Eu and Tb presumably exists on/in the nanosheets as impurities such as $RE(OH)_3$ and/or $RE(CH_3COO)_3$. Fig. 5 shows an AFM image of [Eu–Tb–multi-sheet]$_3$. It was found that the nanosheets

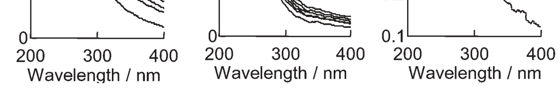

Fig. 4 UV-vis absorption spectra of layered films; (A) [Eu–$Ti_{1.81}O_4$]$_n$, (B) [Tb–Nb_6O_{17}]$_n$ and (C) [Eu–Tb–multi-sheet]$_n$.

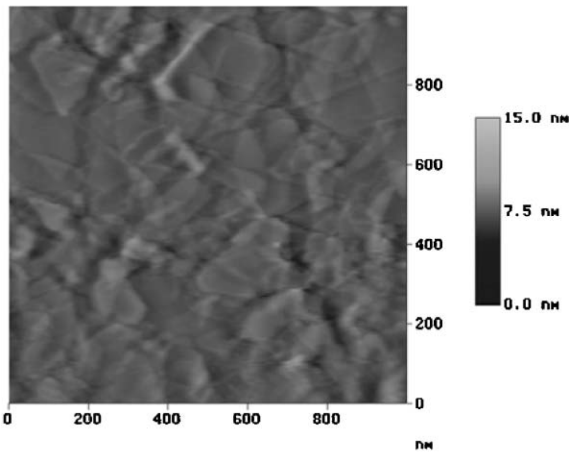

Fig. 5 AFM image of [Eu–Tb–multi-sheet]$_3$.

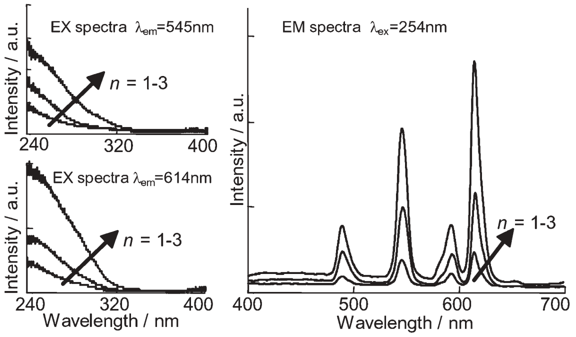

Fig. 6 Excitation and emission spectra of [Eu–Tb–multi-sheet]$_n$ (n = 1–3).

were laminated by the LBL process. According to the results, we confirmed that the [Tb–Eu–multi-sheet]$_n$ film was able to be prepared by the LBL technique.

Fig. 6 shows the excitation and emission spectra of [Tb–Eu–multi-sheet]$_n$ (n = 1–3). In the emission spectra monitored at 254 nm, the emission peaks assigned to the Eu^{3+} and Tb^{3+} ions were obtained. With increasing sequence number, the excitation and emission intensity were increased, indicating that the Eu^{3+} and Tb^{3+} ions were laminated with nanosheets. The shapes of the excitation spectra of [Tb–Eu–multi-sheet]$_n$ monitored under 614 and 545 nm were almost the same as those of Eu–$Ti_{1.81}O_4$ and Tb–Nb_6O_{17}, respectively. According to the results, it was found that the photoluminescence property of Eu^{3+} ions in the interlayer between $Ti_{1.81}O_4$-sheets is almost independent of that of Tb^{3+} ions between Nb_6O_{17}-sheets.

The increase in the emission intensity with respect to the increasing number of layers deviates slightly from linearity. One of the reasons might be the inhomogeneous size distribution of the nanosheets,[11] which might affect the homogeneous adsorption of nanosheets and full coverage of the substrate surface.

We have already reported that coordinating water molecules in Eu–$Ti_{1.81}O_4$ play an important role in the luminescent properties of Eu^{3+}.[9] Fig. 7 shows how humidity controlled experiments on [Tb–Eu–multi-sheet]$_6$ affect its photoluminescence property at room temperature. The as-prepared sample gave a high-intensity peak on Eu^{3+} emission and excitation spectra at 100% humidity, while the film conditioned at 5% humidity produced peaks with much lower intensity. However, the variation in humidity has less impact on the photoluminescence properties of the Tb^{3+} ion. It is expected that the electrons and holes migrating in $Ti_{1.81}O_4$-sheets move simultaneously through the surrounding water molecules to the interlayer Eu^{3+} to yield emission rather than giving radiationless quenching *via* energy transfer to OH vibration on the water molecules. Although the detailed mechanism about the role of water on the luminescence properties of the Eu^{3+} in the $Ti_{1.81}O_4$-sheets' interlayer region was unclear, it was revealed that the [Tb–Eu–multi-sheet]$_n$ films vary the emission color according to the surrounding humidity. These layered films of heterogeneous nanosheets with rare earth ions are expected to be the base materials of optical devices and sensors.

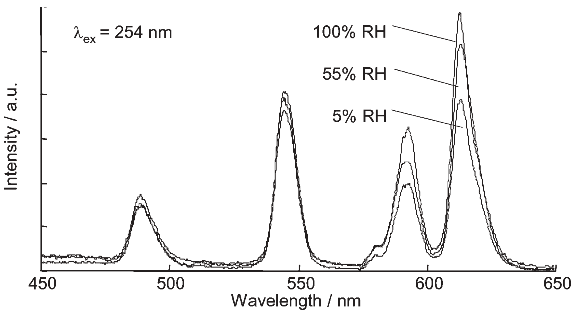

Fig. 7 The humidity dependence of the emission spectra of [Tb–Eu–multi-sheet]$_3$.

In summary, the layered films of heterogeneous nanosheets intercalated with rare earth ions were able to be prepared by a LBL technique and the photoluminescence properties were strongly dependant on the combination of nanosheets: [Tb–Eu–multi-sheet]$_n$ exhibited both red and green luminescence and varied the emission color according to the surrounding humidity.

This work was supported by the Core Research for Evolutional Science and Technology (CREST) program of the Japan Science and Technology Co. (JST) and a Grant-in-Aid for Scientific Research (no. 440, Panoscopic Assembling and High Ordered Functions for Rare Earth Materials, and no. 15350123) from the Ministry of Education, Culture, Sports, Science, and Technology.

Notes and references

1 T. Sasaki and M. Watanabe, *J. Am. Chem. Soc.*, 1998, **120**, 4682.
2 A. Kudo, A. Tanaka, K. Domen, K. Maruya, K. Aika and T. Onishi, *J. Catal.*, 1988, **111**, 67.
3 W. Sugimoto, O. Terabayashi, Y. Murakami and Y. Takatsu, *J. Mater. Chem.*, 2002, **12**, 3814.
4 U. Unal, Y. Matsumoto, N. Tanaka, Y. Kimura and N. Tamoto, *J. Phys. Chem. B*, 2003, **107**, 12680.
5 E. R. Kleinfeld and G. S. Ferguson, *Science*, 1994, **265**, 370.
6 M. Fang, D. M. Kaschak, A. C. Sutorik and T. E. Mallouk, *J. Am. Chem. Soc.*, 1997, **119**, 12184.
7 T. Sasaki, Y. Ebina, M. Watanabe and G. Decher, *Chem. Commun.*, 2000, **21**, 2163.
8 H. Xin, R. Ma, L. Wang, Y. Ebina, K. Takada and T. Sasaki, *J. Appl. Phys. Lett.*, 2004, **85**, 4187.
9 Y. Matsumoto, U. Unal, Y. Kimura, S. Ohashi and K. Izawa, *J. Phys. Chem. B*, 2005, **109**, 12748.
10 K. L. Frindell, M. H. Bartl, M. R. Robinson, G. C. Bazan, A. Popitsch and G. D. Stucky, *J. Solid State Chem.*, 2003, **81**, 172.
11 K. Izawa, T. Yamada, U. Unal, S. Ida, O. Altuntasoglu, M. Koinuma and Y. Matsumoto, *J. Phys. Chem. B*, 2006, **110**, 4645.